RESEARCH ARTICLE

Cullin-5 and cullin-2 play a role in the development of neuromuscular junction and the female germ line of *Drosophila*

CHAMPAKALI AYYUB*

Department of Biological Sciences, Tata Institute of Fundamental Research, Homi Bhabha Road, Mumbai 400 005, India

Abstract

Cullins confer substrate specificity to E3-ligases which are multi-protein complexes involved in ubiquitin-mediated protein degradation or modification. There are six cullin genes in *Drosophila melanogaster*. We have raised an antibody against Cul-5 and demonstrated that it expresses in neuronal and non-neuronal cells throughout development. In the embryonic tracheal system, Cul-5 is enriched at fusion sites together with E-Cadherin and Fasciclin III. Mutations of *cul-5* do not affect tracheal development but do show defects in the organization of synaptic boutons at the larval neuromuscular junction where the protein is expressed in a subset of motoneuron terminals. Loss of function of another *cullin* gene '*cul-2*' results in similar defects at the larval neuromuscular junction although *cul-2;cul-5* double mutants do not show an enhanced phenotype. Both *cul-2* and *cul-5* mutants show similar aberrations in the development of female germ line. Our results suggest that both of these cullin proteins participate in similar developmental processes.

[Ayyub C. 2011 Cullin-5 and cullin-2 play a role in the development of neuromuscular junction and the female germ line of *Drosophila*. *J. Genet.* **90**, 239–249]

Introduction

The role of post-translational modifications in regulation of protein function is increasingly being recognized. Covalent attachment of 76 amino acid polypeptide, ubiquitin (Ub), to the lysine residues of target proteins can serve as a signal either for a degradative (Glickman and Ciechanover 2002) or a nondegradative modification (Welchman *et al.* 2005) depending on the number of residues added. Substrate specificity is conferred by an E3-ligase, a multiprotein complex. Of the four types of E3-ligases identified so far, the Skp1–Cullin-F-box/Elongin C-Cullin–SOCS box (SCF/ECS) complexes are the best studied. Cullins are known to bind to Skp1 or Elongin C, which with the help of F-box or SOCS box proteins attaches to the substrate. The highly conserved C-terminal domain of cullin protein binds to a RING-finger containing protein (viz. Hrt1/ Roc1/ Rbx1) (Feldman *et al.* 1997; Skowyra *et al.* 1997).

Of the six *cullin* (*cul*) genes identified in *Drosophila melanogaster, cul-1* and *cul-3* have been shown to have important roles in SCF-based degradation of proteins belonging to different signalling pathways (Filippov *et al.* 2000; Ou *et al.* 2002, 2003; Mistry *et al.* 2004). Both Cul-1 and Cul-3 regulate the level of Cubitus interruptus, a member of the Hedgehog signalling pathway. In addition, Cul-3 plays multiple roles in patterning, sensory system development and survival (Mistry *et al.* 2004). A testis-specific isoform of Cul-3, in combination with the small RING protein Roc1b and BTB-Kelch protein Klh10, acts as an ubiquitin ligase to regulate caspase activation during spermatogenesis (Arama *et al.* 2007). On the other hand, Cul-1-based E3-ligase is essential for determination of the exact number of nurse cells during oogenesis in *Drosophila* (Ohlmeyer and Schupbach 2003).

The role of Cul-5 in *Drosophila* is less well understood. Several studies in cell culture and mammalian systems link Cul-5 to cell cycle regulation (Querido *et al.* 2001; Fay *et al.* 2003; Van Dort *et al.* 2003). We had previously used an insertional mutation upstream of *Drosophila cul-5* to show that gain of function affects cell proliferation, cell fate determination and survival during sensory system development (Ayyub *et al.* 2005). Later, Reynolds and co-workers identified a null allele of *cul-5* and found that the total loss-of-function mutation does not affect viability but leads to reduced female fecundity (Reynolds *et al.* 2008). Cul-5 has been recently implicated in germ line maintenance, follicular morphogenesis and regulation of cyst divisions within the ovary (Kugler *et al.* 2010). These pleiotropic phenotypes suggest multiple targets of cullin-5 which still need to be identified.

*E-mail: kali@tifr.res.in.

Keywords. *Drosophila*; *cullin-5*; *cullin-2*; trachea; bouton; ovary.

Although mutations of *cul*-2 gene in *Drosophila* are known, the role of this gene is still unclear. Studies in mammalian cell culture have shown that a Cul-2-based complex containing VHL-box proteins degrades hypoxia-inducible factor-α (HIF-α) important for angiogenesis (Maxwell *et al.* 1999). In *Caenorhabditis elegans, cul-2* plays an important role in cell cycle regulation during germline proliferation (Feng *et al.* 1999; Sasagawa *et al.* 2007). Cul-2 can be compensated by Cul-5 and double mutants of *cul-2* and *cul-5*, give rise to defects in oogenesis which is not seen in the single mutants (Sasagawa *et al.* 2007).

In this paper, we use immunocytochemistry to describe the expression pattern of *Drosophila* Cul-5; using an antibody against Cul-5, our results demonstrate that the protein is widely expressed in multiple tissues during development. We focus on two tissues—the embryonic trachea and the larval neuromuscular junction (NMJ) where Cul-5 shows a striking expression pattern. In the developing trachea, Cul-5 is enriched in fusion cells together with DE-Cadherin and FasIII. Absence of Cul-5, however, does not affect tracheal development suggesting a possible redundant function. In the larval NMJ, Cul-5 is expressed in a subset of synaptic boutons and is enriched postsynaptically. Mutations of *cul-5* as well as *cul-2* affect the regulation of bouton number at NMJ. We provide evidence for similar roles of Cul-5 and Cul-2 at NMJ and during oogenesis, although evidence for their possible genetic interaction is still lacking.

Materials and methods

Drosophila stocks

Df(3R)3450/TM6B, Tb^1 (98E3;99A6-A8), y^1,w*;D* gl^3/TM3, P{GAL4-Kr.C}DC2, P{UAS-GFP.S65T}DC10 Sb^1,y^1w^{67c23}; P{EPgy2}cul-$5^{EY21463}$ ($cul\text{-}5^{EY}$), y^1w^{67c23}; P{EPgy2}cul-$2^{EY09124}$($cul\text{-}2^{EY}$), P{EPgy2}cul-$2^{EY00051}$, P{PZ}cul-2^{02074} cn^1/CyO; ry^{506} ($cul\text{-}2^{PlacZ}$), and y^1w^1; Ki^1P{ry$^{+t7.2}$Δ2–3}99B were obtained from the Bloomington *Drosophila* Stock Center, Indiana, USA. The RNAi-line w^{1118};P{GD8913}v19297 (abbreviated as $cul\text{-}2^{RNAi}$) corresponding to the *cul-2* gene was obtained from the Vienna *Drosophila* RNAi Center Vienna, Austria. Canton special (CS) flies were used as wildtype control. To avoid the effect of background mutations in the $cul\text{-}5^{EY}$ stock, we examined phenotypes in *trans* with a deficiency uncovering the gene. Flies were grown at 25°C on standard *Drosophila* medium.

Generation of excision lines

To generate lines where the transposon was excised, virgins of $cul\text{-}5^{EY}$/TM3-*Sb* were crossed to males of y^1w^1; Ki^1P{ry$^{+t7.2}$Δ2–3}. The 'Jumpstarter' males were mated to w^{1118};TM3-*Sb*/ TM6-*Tb*. Since the EY element carries a mini-white gene, progeny of this cross was screened for white-eyed flies. One precise excision line ($cul\text{-}5^{exB}$) was isolated after screening 6836 males.

Generation of antibodies and immunostaining

A 529-bp fragment of *cul-5* cDNA was PCR-amplified from an embryonic cDNA library (a gift from Dr N. Brown, University of Cambridge, UK) using a set of primers (forward: 5-*Eco*RI-ATGCTACGGGCAAT-3 and reverse: 5-*Sal*I-TCAGGAGGCTGCAG-3). The PCR product was inserted into expression vector pATH11 (Koerner *et al.* 1991). Polyclonal serum against this fusion protein was raised in rats and was used at 1 : 40 dilution on tissues and at 1 : 200 dilutions in Western blots.

Embryos were fixed in 4% paraformaldehyde-saturated heptane, devitellinized in methanol and stained according to the protocol of Gould *et al.* (1990). For staining imaginal discs from third instar larvae, fixation and washes were followed as described in Ray and Rodrigues (1995). To stain boutons at NMJ, wandering third instar larvae were dissected in ice-cold Ca^{2+}-free saline (128 mM NaCl, 2 mM KCl, 21.5 mM $MgCl_2$, 5 mM 4-(2-hydroxyethyl)-1-piperazineethanesulphonic acid (HEPES), pH 7.3, 36 mM sucrose), fixed in 3.5% paraformaldehyde in PBS (137 mM NaCl, 2.7 mM KCl, 1.5 mM KH_2PO_4, 8 mM Na_2HPO_4, pH 7.3) for 30 min and processed for antibody staining as described previously (Budnik *et al.* 1990; Estes *et al.* 1996). Briefly, the preparation was first blocked in PBS containing 0.1% triton X-100 (PTX) with 2% bovine serum albumin (PBTX) for 1 h at room temperature. Samples were incubated overnight in primary antibody in PBTX at 4°C and in secondary antibody for 1 h at room temperature. The following primary antibodies used were from Developmental Studies Hybridoma Bank, University of Iowa, Iowa, USA: rat anti-DE-Cadherin (1 : 20), mouse anti-FasIII (1 : 5), mouse anti-FasII (1 : 5), mouse anti-β-galactosidase (40–1a; 1 : 50) and 2A12 (1 : 10). anti-HRP (1 : 10,000) antibody was obtained from Sigma, St. Louis, USA. Human anti-Cul-5 (1 : 25) antibody was from Abcam Laboratories, Cambridge, USA and was raised against a synthetic peptide corresponding to a region between amino acids 526–575 of human Cul-5. Secondary antibodies conjugated to Alexa Fluor-488, -568 and -647 (Molecular Probes, Bangalore, India) were used at 1 : 400 dilution. In some experiments, the primary antibodies were detected after amplification with biotinylated secondary antibodies and fluorescent-dye conjugated-streptavidin (Vector Labs, Burlingame, USA).

Ovaries were dissected in PBS, fixed for 1 h in 4% paraformaldehyde in PBS, rinsed with PBS with 0.3% triton X-100 (PTX 0.3%) and then incubated for 15 min in 5 μg/mL Hoechst. After washing with PTX 0.3%, ovaries were teased apart and mounted in anti-fading mountant (Vectashield, Vector Labs, Burlingame, USA).

Except for the images of wildtype NMJ double-labelled with Fas-II and Cul-5 antibodies and mutant NMJ double-labelled with HRP and Cul-5 antibodies, where Olympus FV1000 confocal microscope and Olympus Fluoview version 1.4a program were used, samples were imaged with an apotome (Zeiss) and processed using ImageJ (http://rsb.info.nih.gov/ij/; Wayne Rasband, National Institute of Health,

Bethesda, USA) and Adobe Photoshop 7.0. Statistical analysis was performed and barcharts were generated using Excel. Statistical significance between two groups was assessed using Student's unpaired *t*-test.

Results

Sequence comparison among six cullin proteins of *Drosophila* demonstrates significant homology over the entire length of the proteins being most significant at the C-terminus. Figure 1A shows the N-terminal region of this comparison and highlights a stretch of 176 amino acids (of which 64 are unique to Cul-5) used to generate a polyclonal antibody (demarcated with red arrowheads in figure 1A). The serum recognizes a 93-kDa band corresponding to the expected size of Cul-5 on Western blot of *Drosophila* embryo extract (figure 1G).

Immunostaining of embryos reveals a widespread expression of Cul-5 in the developing nervous systems (figure 1, B–D). The protein continues to express in the central nervous system (CNS) of larva and can be detected in somata of most cells in the ventral nerve cord (figure 1E; white arrowheads in the inset). Staining was also observed in the eye imaginal discs of third instar larvae behind the morphogenetic furrow (indicated by red dotted line; figure 1F). The 'boxed-in region' in figure 1F is enlarged in the inset to highlight staining in photoreceptor cells (white arrowheads). Expression in antennal disc is restricted to a few cells within the anlage of the third antennal segment (red arrowhead; figure 1F).

Cul-5 protein is enriched at fusion sites in the developing embryonic trachea

Wildtype embryos of *Drosophila* stained with a lumen-specific antibody, mAb2A12, reveal the basic tracheal

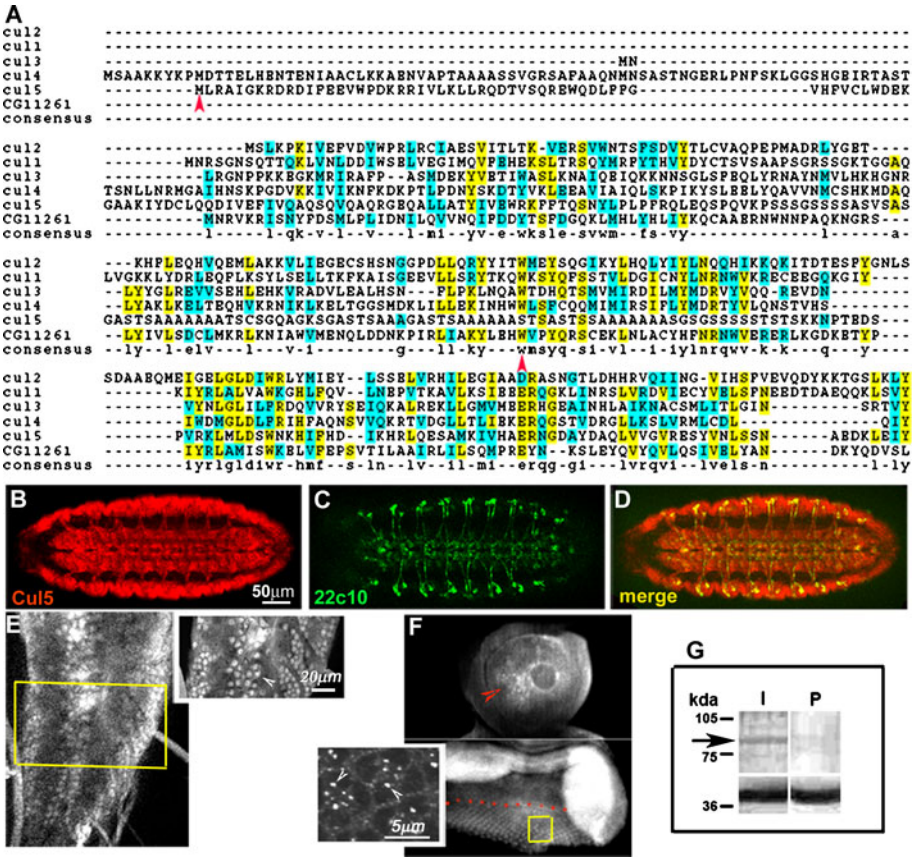

Figure 1. Sequence comparison among cullin proteins of *Drosophila* and expression of Cul-5 in embryo and larva. (A) Comparison of the N-terminal regions of the six *Drosophila* cullin proteins. The fragment from Cul-5 protein used for antibody generation is marked with red arrowheads. (B–D) Wildtype embryo double-stained with anti-Cul-5 (B) and neuron-specific antibody mAb22c10 (C). (D) Merged images show that Cul5 is present in the CNS. Scale bar = 50 μm (B–D). (E) Expression persists in larval ventral nerve cord (white arrowheads in inset showing at a high magnification; scale bar = 20 μm) and (F) eye-antennal disc of third instar larva. Cul5 is present behind the morphogenetic furrow (red dotted line). The yellow boxed-in area (scale bar = 5 μm) is enlarged in the inset to show expression in photoreceptor cells (white arrowheads). In antennal disc, Cul5 expresses in few unidentified cells (red arrowhead) within the anlage of the third antennal segment. (G) Western blot of embryo-extract probed with preimmune (P) and immune-sera (I) against the fusion peptide. The immune sera shows a prominent band at ~93 kDa (arrow). The bottom panel shows a band of ~38 kDa from the same blot which is recognized by both preimmune and immune sera; the equal intensity of the bands indicates equal loading of samples.

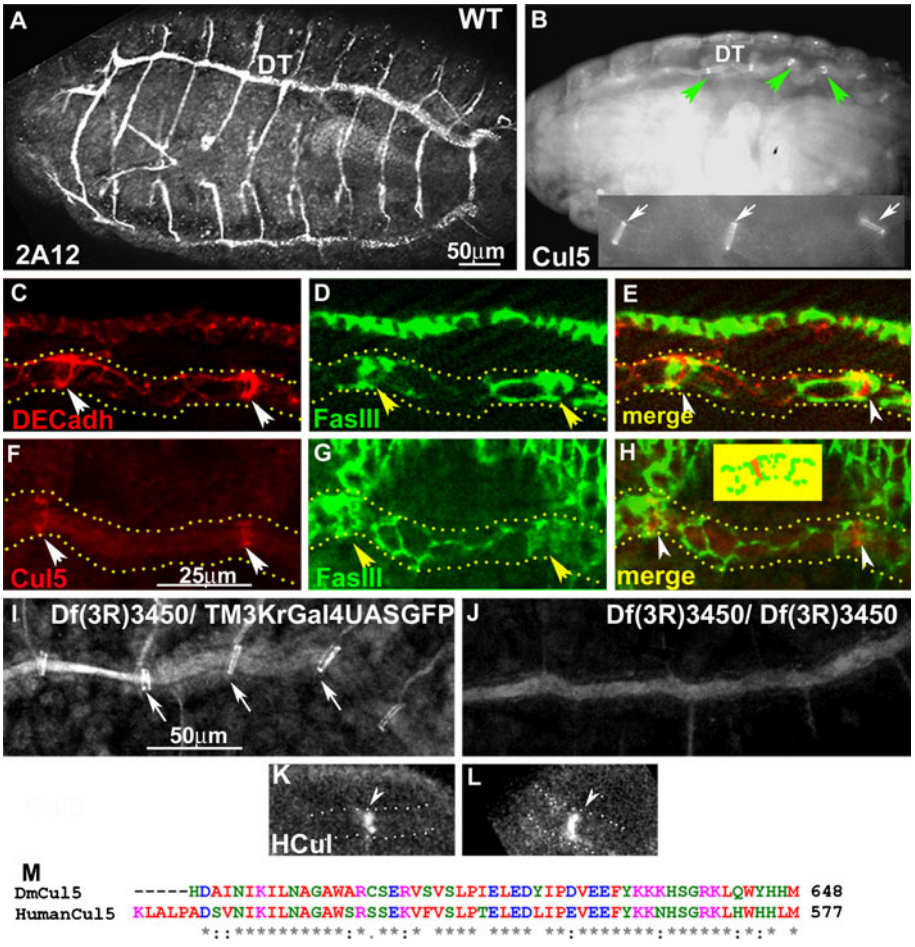

Figure 2. Cul-5 expresses at fusion sites in dorsal trunk. (A) Dorsal view of wildtype embryonic trachea stained with mAb2A12 that stains the tracheal lumen. The dorsal trunk (DT) runs along the length of the embryo. (B) Dorsal view of the wildtype embryonic tracheal system at stage 16 stained with anti-Cul-5 antibody. Rings of Cul-5 (green arrowheads) are detected in dorsal trunk (DT); inset at high magnification reveals a doublet in each ring (white arrows). Scale bar = 50 μm (A–B). (C–L) Enlarged view of segments of the dorsal trunk of wildtype embryos at stage 16. (C–H) Boundaries of the trachea are demarcated in dotted lines. Labelling with anti-DE-Cadherin (C) (white arrowheads) and anti-FasIII (D) (yellow arrowheads). Merged image (E) shows that the rings of DE-Cadherin (white arrowheads) are localized at the fusion site of two fusion cells which express DE-Cadherin and FasIII juxtaposed to each other. (F–H) Labelling with antibodies against Cul-5 (F; white arrowheads) and FasIII (G; yellow arrowheads). Merged image (H) shows that Cul-5 localizes at the fusion site (white arrowheads) of two growing tracheal cells expressing FasIII. Diagram indicates the localization of Cul-5 (red) and FasIII (green). (I–J) Enlarged view of segments of the dorsal trunk of embryos of the genotype Df(3R)3450(98E3;99A6-A8)/TM3SbKrGal4UASGFP (I) and Df(3R)3450(98E3;99A6-A8) (J) stained with anti-Cul-5 and anti-GFP. The GFP panels are not shown but allow identification of Df(3R)3450/TM3SbKrGal4UASGFP heterozygotes. Cul-5-specific rings, (I; white arrows), are absent in embryos homozygous for deficiency Df(3R)3450, which lack the *cul-5* gene (J). Nonspecific staining persists within the tracheal lumen. Scale bar = 50 μm (I–J). An antibody raised against a region of human Cul-5 (HCul) with high homology to the *Drosophila* protein (M) also stains rings (white arrowheads) in the dorsal trunk of the trachea (K and L). Scale bar = 25 μm (C–H; K–L).

architecture at stage 16 (figure 2A). Embryonic tracheal development in *Drosophila* starts in individual hemisegments when a specific number of cells undergo change in cell shape to form tubes and migrate under the influence of the fibroblast growth factor receptor, breathless (Btl) (Klambt *et al.* 1992; Sutherland *et al.* 1996; Ghabrial *et al.* 2003). To form a continuous network, specific branches from each hemisegment connect to their neighbours with the help of a fusion cell located at the tip of each growing branch. A contact between the fusion cells triggers enrichment of cell adhesion molecule DE-Cadherin to establish an extracellular junction and formation of a continuous lumen passing through them. This is followed by an enrichment of FasIII which also forms a ring at the contact site (Samakovlis *et al.* 1996b; Tanaka-Matakatsu *et al.* 1996). FasIII is a component of septate junction of tracheal cells while the apically located adherens junction contains DE-Cadherin (Samakovlis *et al.* 1996a).

In the dorsal trunk, Cul-5 starts accumulating at the fusion sites from stage 14 onwards and at stage 16 is strongly enriched in prominent rings at regular intervals (green arrowheads in figure 2B; white arrows in the inset showing

magnified dorsal trunk). To localize the domains of expression of Cul-5 relative to well-characterized tracheal markers, we stained embryos at the same stage of development with antibodies against *Drosophila* DE-Cadherin and Fasciclin III.

As expected, DE-Cadherin was observed in rings (figure 2C, white arrowheads) indicating the site of fusion of the tip cells. FasIII is also enriched at the fusion sites (figure 2, D & G; yellow arrowheads) closely juxtaposed with the expression domains of DE-Cadherin (figure 2E). Double-labelling with anti-FasIII (figure 2G, yellow arrowheads) and anti-Cul5 (figure 2F, white arrowheads) revealed that Cul-5 protein is strongly enriched at the fusion site where FasIII protein is enriched (figure 2H; diagram in inset depicts Cul-5 in red and FasIII in green). These observations together favour the conclusion that Cul-5 is enriched at the same position as DE-Cadherin and FasIII which have been shown to play significant roles in the fusion process (Samakovlis *et al.* 1996b; Tanaka-Matakatsu *et al.* 1996). We had previously demonstrated that Cul-5 mRNA is first detected at stage 13 of embryogenesis in clusters of cells corresponding in morphology and position to the precursors within the tracheal placode (Samakovlis *et al.* 1996a; Ayyub *et al.* 2005).

We verified the authenticity of anti-Cul-5 antibody by staining embryos homozygous for deficiency Df(3R)3450 (98E3; 99A6–A8) which uncovers the *cul-5* locus. Such embryos showed an absence of anti-Cul-5 immunoreactivity at the tracheal rings although there is significant background staining within the tracheal lumen (figure 2J). Siblings of genotype Df(3R)3450/TM3*SbKr*-Gal4UASGFP showed staining comparable to that of the wildtype (figure 2I, white arrows). In order to verify the expression of Cul-5 in the tracheal rings, we used an independent polyclonal serum raised against synthetic peptide corresponding to a region of human Cul-5 that bears a high level of identity with *Drosophila* Cul-5 (figure 2M). The tracheal rings that we described using *Drosophila* anti-Cul-5 were also revealed using this antibody (figure 2, K&L).

Staining of embryos deficient for *cul-5* with mAb2A12 did not reveal any defects in tracheal morphology and the distribution of DE-Cadherin and FasIII in them were normal (data not shown). The role of Cul-5 during tracheal development remains elusive and it is clearly not essential for sequestering DE-Cadherin and FasIII at the fusion sites.

Cul-5 expresses at the neuromuscular synapses

In the *Drosophila* larval body wall, synaptic boutons can be classified depending on their size, shape and the neurotransmitter they contain (Keshishian *et al.* 1996). Glutamate is the excitatory neurotransmitter for all motor axons, while some terminals co-express octopamine (Atwood *et al.* 1993) and peptide transmitters like insulin-like peptide (Johansen *et al.* 1989). The role of ubiquitin-mediated protein degradation in sculpting the NMJ has been reported for *Drosophila* (Speese *et al.* 2003; Watts *et al.* 2003) and *Aplysia* (Zhao *et al.* 2003). In our previous study (Ayyub *et al.* 2005), we reported an increase in bouton number in larval NMJ of the hypomorphic excision alleles *cul-5*^{x2} and *cul-5*^{x29} in *trans* with the deficiency Df(3R)3450. Mutants with elevated Cul-5 levels (*elav*-Gal4::*cul-5*^{EP3390}) also showed the same defects.

To investigate this further, we stained the NMJ of third instar larvae with anti-Cul-5 and a pre-synaptic marker anti-HRP (Gramates and Budnik 1999). Expression of Cul-5 is

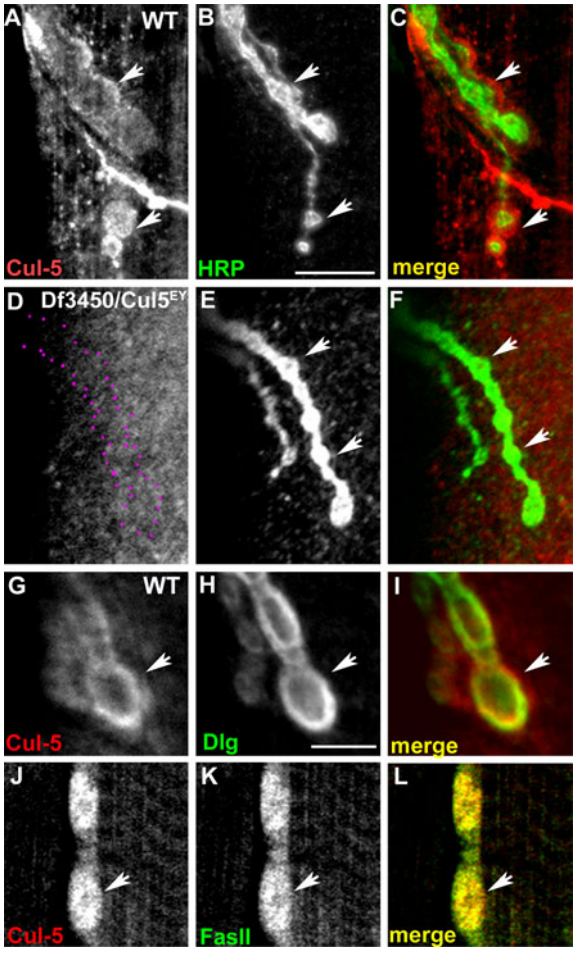

Figure 3. Cul-5 is localized at the larval NMJ. (A–F) NMJs of wildtype (A–C) and Df(3)3450/*cul-5*^{EY} (D–F) larvae at muscles 6 and 7 labelled with anti-Cul-5 (A and D; red in merged image) and the presynaptic marker anti-HRP (B and E; green in merged image). (A–C) In wildtype larvae Cul-5 expresses in type-I boutons (white arrows A and B) and appears to be enriched in the region of the bouton excluded by the anti-HRP staining (C; white arrows). (D–F) Cul-5 does not stain boutons in the Df(3)3450/*cul-5*^{EY} mutant animals (D); the position of the NMJ is indicated by dotted lines. Staining persists in the muscles of Df(3)3450/*cul-5*^{EY} indicating that this is nonspecific. Scale bar = 10 μm (A–F). (G–L) Enlarged view of synaptic boutons stained with anti-Cul-5 (G, I, J, L; red in merges) and Dlg (H and I; green in merges). Cul-5 is localized together with Dlg suggesting its postsynaptic enrichment (white arrow in G–I). (J–L) Labelling with anti-Cul-5 (J, L; red in merges) and anti-FasII (K, L; green in merges). FasII expresses at both presynaptic and postsynaptic regions of NMJ. Colocalization of Cul-5 with FasII is an evidence for its expression in both presynaptic and postsynaptic regions of the synapses. Scale bar = 5 μm (G–L).

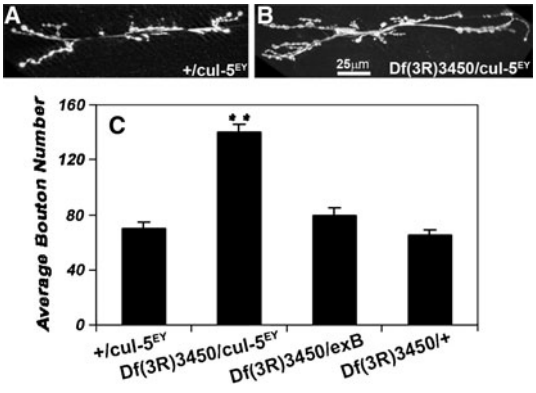

Figure 4. *cul-5* regulates synaptic growth at larval NMJ. (A–B) HRP-labelled NMJ in muscles 6 and 7 of Df(3)3450(98E3;99A6-A8)/*cul-5*^{EY} (B) show an increased number of boutons and branching with respect to control +/*cul-5*^{EY} (A). The NMJs of control Df(3)3450/+ animals are comparable to (A) and is not shown. Scale bar = 25 μm (A–B). (C) Quantitation of defect in NMJ of *cul-5*^{EY} mutant and the revertant *cul-5*^{exB}. Boutons on muscles 6 and 7 were counted over 20 hemisegments from abdominal segment A2 for each of the following genotypes: +/*cul-5*^{EY}, Df(3)3450/*cul-5*^{EY}, Df(3)3450/*cul-5*^{exB} and +/Df(3)3450). Bars in histogram represent the mean and standard error of the mean. The comparison of bouton numbers in the loss-of-function animals with controls showed significant increase (** $P < 0.001$).

enriched in a subset of HRP-expressing glutamatergic type I boutons as shown for muscles 6 and 7 (figure 3, A–C, white arrows). We showed that the immunoreactivity in the boutons was specific by staining *cul-5*^{EY} in *trans* with Df(3R)3450 with the same set of antibodies. The staining of anti-Cul-5 in synaptic boutons of the transheterozygote animals was abolished but staining in the musculature remained suggesting that the latter was nonspecific (figure 3, D–F).

While Cul-5 expresses throughout the synaptic boutons, its localization is not uniform; higher levels are seen in regions excluded by anti-HRP staining (arrowheads figure 3C). This suggests a postsynaptic enrichment, which we confirmed by double-labelling the NMJ with an antibody against Discs large (Dlg) known to be enriched in postsynaptic densities (Lahey *et al.* 1994; Guan *et al.* 1996; Packard *et al.* 2002) (figure 3, G–I). Co-localization of Cul-5 with Fasciclin II (FasII) which expresses on both presynaptic and postsynaptic regions of the NMJ (Schuster *et al.* 1996), confirms that the protein is found on both presynaptic and postsynaptic regions of the synaptic bouton (figure 3, J–L). However, the protein is strongly detected on the postsynaptic side of the neuron–muscle synapse.

Our previous results, where we used weak excision mutants of the *Cul-5* gene to demonstrate that loss of function of *cul-5* leads to defects in synapse development (Ayyub *et al.* 2005), were not unequivocal as a later study by Reynolds and co-workers with those mutants showed that the homozygous mutants still produced normal levels of mRNA. They also reported a total loss of function but viable allele, *cul-5*^{EY}, which did not produce any Cul-5 protein as detected in immunoblots (Reynolds *et al.* 2008). When stained with anti-HRP, larvae of *cul-5*^{EY} in *trans* with the deficiency Df(3R)3450, showed a significant increase in bouton number (figure 4B) compared to controls (figure 4A). In control animals (+/*cul-5*^{EY}), we counted 65 ± 3 (n = 20 hemisegments) boutons on muscles 6 and 7 from abdominal segment A2; in the Df(3R)3450/*cul-5*^{EY} this number was increased two-fold to 139 ± 6 (n = 20 hemisegments; $P < 0.001$). A similar increase was observed when mutants were compared to the Df(3R)3450/+ control (figure 4C; $P < 0.001$). In addition to the increased bouton number, the organization of the synaptic structures in the mutant appeared to be much more elaborate (figure 4B) with respect to the number of branches as compared to controls (figure 4A). The average number of branches counted from muscles 6 and 7 of abdominal segment A2 in Df(3R)3450/*cul-5*^{EY} was 21.2 ± 1.2 (n = 20 hemisegments). It was significantly higher ($P < 0.001$) than the average number of branches 9.6 ± 0.6 (n = 20 hemisegments) in control (+/*cul-5*^{EY}) larvae. This suggests that the loss-of-function mutation of *cul-5* gives rise to branching defects too. The *cul-5*^{EY} mutation results from an insertion of a *P*-element in the second intron of the gene (Reynolds *et al.* 2008). We generated a precise excision of the *P*-element, *cul-5*^{exB}. Larvae of *cul-5*^{exB} in *trans* with the deficiency Df(3R)3450 did not show any defect in synaptic boutons (figure 4C). This supports the finding that defects in Cul-5 function affect regulation of branching and bouton formation at the NMJ.

Complete loss-of-function alleles of *cul-5* (*cul-5*^{EY}) are viable and the defects seen are relatively subtle suggesting the possibility that other *cullin* genes may play overlapping roles during development. Based on the evidence in *C. elegans* that Cul-5 interacts with Cul-2 during ovary development (Sasagawa *et al.* 2007), we set out to examine the roles of *cul-2* in tissues where a role for *cul-5* has been demonstrated.

Cullin-2 may act together with Cul-5 in several tissues

Cul-5 and Cul-2 have been studied in mammalian systems where it has been shown that both of them interact with the adaptor proteins, Elongin B and Elongin C, and some B–C box proteins and function as an E3 ligase (Duan *et al.* 1995; Kibel *et al.* 1995; Kamura *et al.* 2004; Babon *et al.* 2008). Similarly, the *Drosophila* Cul-2 combines with the Elongin B, Elongin C-Rbx1–VHL complex and regulates the level of HIF1a in an ubiquitin-dependent process (Lisztwan *et al.* 1999; Aso *et al.* 2000; Babon *et al.* 2008). There is a high degree of homology between Cul-2 and Cul-5 proteins particularly at the C-terminal end (data not shown).

Figure 5A depicts the organization of the *cul-2* locus (http://flybase.org) with arrowheads showing positions of the P-element insertions in the two mutants. *cul-2*^{EY} has an insertion in the first intron and homozygous adults are viable. The enhancer trap strain *cul-2*^{PlacZ} carries a P-element

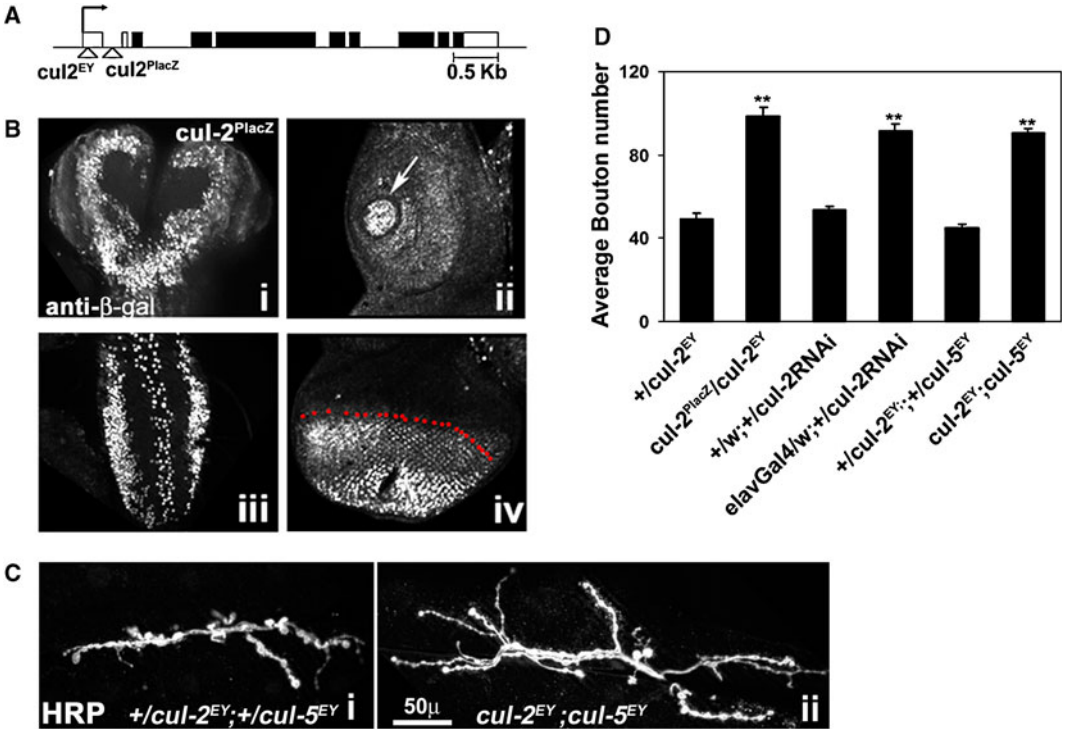

Figure 5. Characterization of *cul-2* locus: (A) schematic of the genomic region of *cul-2* locus. The open and the dark boxes indicate exons and open reading frame, respectively. The straight lines indicate introns. Start of transcription site has been shown by an arrow and the arrowheads mark the positions of *P*-element insertions. (B) In third instar larvae of cul^{PlacZ}, expression of β-galactosidase was observed in brain (i), ventral nerve cord (iii) and eye-antennal discs (ii and iv). In eye-discs (iv), it expresses in the differentiated cells behind the morphogenetic furrow (red dotted line) and in antennal disc (ii), it is present in cells (marked by white arrow) that give rise to the arista. (C–D) Quantitation of defects in NMJ of *cul-2* mutant and the double mutant of *cul-2* and *cul-5*. (Ci-ii) HRP-labelled NMJ in muscles 6 and 7 of $cul\text{-}2^{EY}$; $cul\text{-}5^{EY}$ (ii) show an increased number of boutons with respect to control $+/cul\text{-}2^{EY}$; $+/cul\text{-}5^{EY}$ (i). Scale bar = 50 μm boutons on muscles 6 and 7 were counted over 20 hemisegments from abdominal segment A2 for each of the following genotypes: $+/cul\text{-}2^{EY}$, $cul\text{-}2^{PlacZ}/cul\text{-}2^{EY}$, elavGal4-driven $cul\text{-}2^{RNAi}$, $+/w$; $+/cul\text{-}2^{RNAi}$, cul$-2^{EY}/+$; $cul\text{-}5^{EY}/+$ and $cul\text{-}2^{EY}$; $cul\text{-}5^{EY}$. Bars in histogram represent the mean and standard error of the mean. The comparison of bouton numbers in the experimental larvae with their respective controls showed significant increase (** $P < 0.001$).

insertion in the first noncoding exon of the gene (figure 5B) and reports on the normal expression of the gene in the embryonic CNS (http://flyview.unimuenster.de). Using this strain, we detected strong expression of the reporter β-galactosidase in brain lobes (figure 5Bi) and the ventral nerve cord (figure 5, Biii) of third instar larvae. Expression is also detected in the eye-antennal discs in the anlage of adult arista (arrow in figure 5, Bii) and posterior to the morphogenetic furrow (marked by red dotted line in figure 5, Biv) in the developing photoreceptors of the compound eye. This expression pattern is similar to that of Cul-5 (see figure 1F).

To test for an overlap of functions between Cul-2 and Cul-5, we first examined whether mutants of *cul-2* had defects at the NMJ. Transheterozygotes of $cul\text{-}2^{PlacZ}/cul\text{-}2^{EY}$ survive allowing us to stain the body wall muscles of larvae of $cul\text{-}2^{PlacZ}/cul\text{-}2^{EY}$ with anti-HRP. Motor neurons of $cul\text{-}2^{PlacZ}/cul\text{-}2^{EY}$ larvae formed additional synaptic boutons on muscles 6 and 7 (98 ± 4, $n = 20$ hemisegments) compared to $cul\text{-}2^{EY}/+$ controls (49 ± 2, $n = 20$ hemisegments; $P < 0.001$; figure 5, C&D). RNAi-mediated knockdown of *cul-2* function in all neurons (elav-Gal4::UAS-$cul\text{-}2^{RNAi}$) also shows a similar defect as *cul-2* mutants at the larval NMJ. The number of boutons on a single axon (92 ± 3, $n = 20$ hemisegments) were almost double that of +/UAS-$cul\text{-}2^{RNAi}$ controls (53 ± 1; $n = 20$ hemisegments; $P < 0.001$; figure 5D). Double mutant animals of genotype $cul\text{-}2^{EY}$; $cul\text{-}5^{EY}$ were affected although the severity of the defect was not enhanced over that of the single mutants alone (90 ± 2, $n = 20$ hemisegments) as compared to controls -$cul\text{-}2^{EY}/+$; $cul\text{-}5^{EY}/+$ (45 ± 2, $n = 20$ hemisegments; $P < 0.001$). Further, to understand the roles of Cul-5 and Cul-2 in development of the larval NMJ, number of boutons in gain of function of *cul-5* was counted in the background of loss of function of *cul-2*. As compared to the control elavGal4::$cul\text{-}5^{EY00051}$ (127 ± 4, $n = 15$ hemisegments), there was a decrease in the number of boutons in elavGal4::UAS-$cul\text{-}2^{RNAi}$::$cul\text{-}5^{EY00051}$ (92 ± 5, $n = 15$ hemisegments; $P < 0.0001$) but it was comparable to number of boutons observed with elav-Gal4::UAS-$cul\text{-}2^{RNAi}$ (92 ± 3, $n = 20$ hemisegments). These data together do suggest a role for Cul-2 in synapse formation at the larval NMJ and also indicate that Cul-2 and Cul-5 do not seem to act independently during synapse formation.

Role of Cul-5 and Cul-2 in ovary development

cul-5 and *cul-2* alleles have been shown to interact during ovary development in *C. elegans* (Sasagawa *et al.* 2007). Mutants of *cul-5* have already been shown to have defects in germ line cells leading to compromised female fertility (Reynolds *et al.* 2008; Kugler *et al.* 2010) and we found *cul-2*^{EY} homozygous females to be completely sterile. So next we tested the roles of these genes in germ line development in the *Drosophila* ovary.

The *Drosophila* ovary consists of 16 ovarioles, each ovariole is an assembly line for the formation of eggs. In each ovariole, development of the egg starts in germarium with an asymmetric division of stem cells giving rise to a selfrenewing stem cell and a cystoblast. The cystoblast undergoes four mitotic divisions with incomplete cytokinesis producing an egg chamber with 16 cells interconnected by cytoplasmic bridges called ring canals. One of the cells develops into an oocyte and the remaining 15 cells become nurse cells. The egg chamber gets surrounded by a monolayer of follicle cells, buds off from the germarium and undergoes development to become mature egg (Spradling 1993).

We examined β-galactosidase expression in females of the *cul-2*^{PlacZ}/*CyO* strain in an effort to trace the expression of the *cul-2* gene during development of the germ line cells at all developmental stages of the ovary (figure 6A). Figure 6, A–C shows ovarioles stained with an antibody against anti-β-galactosidase (figure 6A) and the nuclear dye Hoechst (figure 6B) suggesting a widespread expression of the *cul-2* gene in all germ line cells (figure 6C).

Results obtained from Hoechst staining of ovaries of mutant *cul-2*^{EY} demonstrated a range of defects manifesting in the number of cells in egg chambers at different stages of development (figure 6, E–G). To quantify the extent of defect in a *cul-2*^{EY}mutants, we examined a minimum of 100 egg chambers which in the wildtype contains 15 nurse cells (figure 6D). The most prominent aberration found in mutant ovaries was egg chambers with extra nurse cells (in 54 out of 100 egg chambers). In about 20 egg chambers, we observed 22 nurse cells (asterisks in figure 6E compared to 6D); while 10 had less than 15 nurse cells (white arrowhead in figure 6G). More severe defects were observed in 15 cases where nurse cells showed signs of degradation (arrow in figure 6F) and two cases in which the oocyte (asterisk in figure 6H) differentiated in the centre of the egg chamber with a normal number of nurse cells surrounding it. The germarium is thinner in most *cul-2* mutant ovarioles (insets in figure 6, D&E), and the terminal filament is absent (compare white arrowhead in inset of figure 6D with 6E). In a smaller number of ovarioles, the interfollicular stalks were also missing (figure 6E compare with arrows in 6D). Hence *cul-2*^{EY} mutant ovaries show pleiotropic defects most of which can be explained by postulating defects in cell cycle regulation.

Similar defects were observed in mutants of *cul-5*^{EY} which include decrease in the number of germ cells (asterisk in figure 6I) and degeneration of nurse cells (white arrow in figure 6I). Ovaries from double mutants of *cul-2*^{EY}; *cul-5*^{EY} showed defects similar to the single mutants alone except

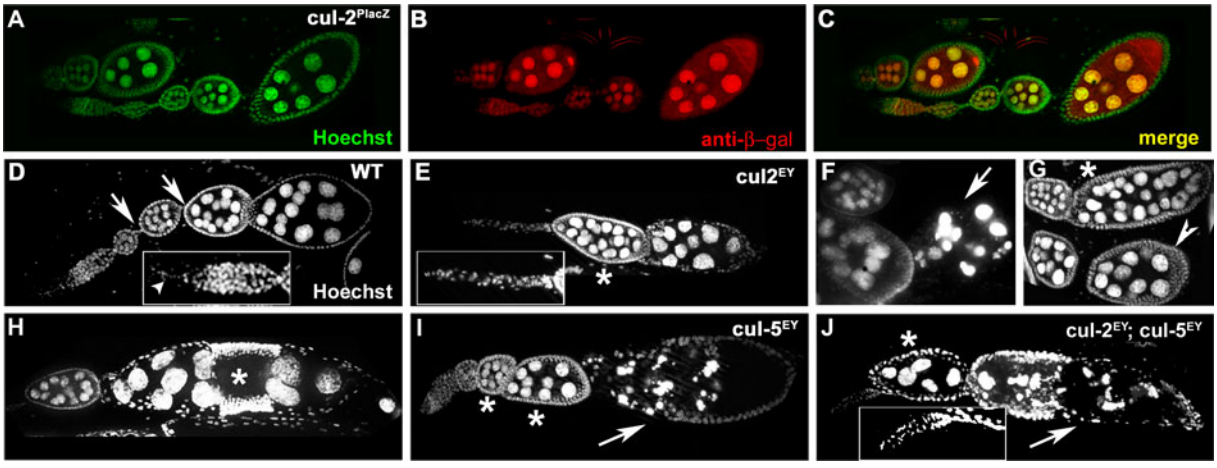

Figure 6. Phenotypes of ovaries from mutants of *cul-2* and *cul-5*. (A–C) Ovaries derived from females with the *cul*^{PlacZ} enhancer trap were stained simultaneously with the nucleus-staining dye Hoechst (A, green) and anti-β-galactosidase (B, red). In the ovarioles of *cul*^{PlacZ} females, germ line cells express β-galactosidase at all stages of development (C, yellow). (D–I) A wildtype ovariole with egg chambers at different stages of development. There are 16 germ line cells in each egg chamber surrounded by a layer of follicle cells and interfollicular stalks are marked by small white arrows (D). (E–H) Egg chambers obtained from *cul-2*^{EY} females have different defects like extra germ line cells (marked by white * in E and G), less number of germ line cells (marked by a white arrowhead in G) and degradation of nurse cells (marked by a white arrow in F). A mutant germarium is thinner and is devoid of a terminal filament (marked by a white arrowhead in inset of D; compare insets in D and E). (H) shows an egg chamber with an oocyte (marked by white *) developing at the centre with nurse cells at both the anterior and posterior of it. (I) An ovariole from *cul-5*^{EY} shows aberrations like less number of germ line cells (marked by white *) and degradation (marked by a white arrow). (I) Ovarioles derived from double mutant *cul-2*^{EY}; *cul-5*^{EY} have egg chambers with less number of germ line cells (marked by white *), degrading nurse cells (marked by a white arrow) and defective germarium (inset).

that a larger proportion (~45%) of egg chambers with fragmented nurse cells were observed (figure 6J). Therefore, as in the case of phenotypes in the larval NMJ, we were able to show that both of these cullin proteins play roles during germ line development but the data did not allow us to conclude whether these proteins acted in the similar cellular process.

Discussion

We have shown that both Cul-5 and the related protein Cul-2 are expressed in multiple tissues during the development of *Drosophila*. Mutants in both these genes lead to defects in the development of the larval NMJ where the numbers of synaptic boutons on the motorneuron are greatly increased over the wildtype. Also both genes affect the development of the *Drosophila* ovary and mutations lead to defects in formation of the germ line cells. In development of both NMJ and ovaries, double mutants of *cul-5* and *cul-2* produced phenotypes comparable to the single mutants. This does not allow us to conclude that the two cullin proteins interact during development although there is a possibility that Cul-5 and Cul-2 could function in the same functional pathway. Homozygous null single mutants as well as *cul-2^{EY};cul-5^{EY}* double mutants are viable as adults but females of *cul-5^{EY}* show greatly reduced fertility and *cul-2^{EY}* and *cul-2^{EY};cul-5^{EY}* show total sterility.

Cul-5 is expressed during development of trachea

Cul-5 is expressed in the tracheal tubes at fusion sites during development. Loss-of-function mutants do not affect the tracheal morphology suggesting that *cul-5* plays a redundant role during development. Other F-box proteins are known to express during tracheal development and could have functions overlapping with Cul-5. The F-box protein Archipelago is a member of the Skip–cullin–F-box–E3-ligase complex that patterns the trachea by promoting ubiquitin-mediated degradation of the basic helix-loop-helix transcription factor, trachealess, in fusion cells. This, in turn, affects the distribution of the Btl receptor thus affecting branch migration (Mortimer and Moberg 2007).

Cul-5 and Cul-2 affect the regulation of synaptic bouton number in the larval motorneurons

Mutations in both *cul-5* and *cul-2* result in an increase of bouton number in motorneurons innervating the NMJ. This phenotype has been observed in several mutants affecting neuronal activity (e.g. *ether-a-go-go, Shaker*) or level of synaptic cell adhesion (e.g. *fasII*) (Budnik *et al.* 1990; Schuster *et al.* 1996). Two well-studied E3-ligases—anaphase promoting complex and highwire—are expressed at the synaptic terminals and their absence results in increases in synaptic growth (Wan *et al.* 2000; van Roessel *et al.* 2004). Highwire, a positive regulator of ubiquitination, is known to control synaptic growth by acting on Wallenda, a member of the MAP kinase signalling pathway (Wu *et al.* 2005; Collins *et al.* 2006). This phenotype is antagonized by Fat facetes, a protein responsible for de-ubiquitination (DiAntonio *et al.* 2001). It needs to be determined whether Cul-5 and Cul-2 function as E3-ligases at the NMJ affecting other key synaptic molecules.

Cul-5 and Cul-2 have multiple roles during oogenesis

Cullin-based E3-ligases are known for their roles in ubiquitin-mediated protein degradation. There are several reports on the involvement of cullins and other members of the cullin-based protein degradation machinery during ovary development in *Drosophila*. Mutation in a gene called *encore* produces 32 germ line cells in an egg chamber indicating an extra round of mitosis in the germ line cells. Encore binds cullin-1, proteosome and cyclin E and controls the exit of germ line cells from mitosis (Ohlmeyer and Schupbach 2003). The F-box protein Slimb is needed in both germ line and follicle cells at different stages of development of ovary in *Drosophila*. It functions in association with cullin-1 in controlling the number of germ line cells and downregulates the decapentaplegic pathway in follicle cells (Muzzopappa and Wappner 2005). The protein Kelch, is known to bind and organize F-actin and has recently been shown to be a part of a Cul3-based E3-ligase required for the growth of ring canals in developing ovaries in *Drosophila* (Kelso *et al.* 2002; Hudson and Cooley 2010).

Loss of function of Cul-5 has been shown to affect oogenesis leading to defects that could be explained by a compromised regulation of cell cycle (Kugler *et al.* 2010). It is well known that exit from cell cycle requires the destruction of cyclins by the ubiquitin proteasome system (Ciechanover *et al.* 2000). This makes it tempting for us to speculate that Cul-2-based and Cul-5-based E3 ligases could act on some aspects of cell number control during ovary development. Kugler *et al.* (2010) have identified gustavas as a substrate of Cul-5. However the interacting partners of both Cul-2 and Cul-5 at the NMJ and the ovary still need to be identified. This work provides background information on the tissue expression of Cul-2 and Cul-5 which will allow further investigation of their molecular role during development.

Acknowledgements

I would like to thank the Bloomington *Drosophila* Stock Centre and the Developmental Studies Hybridoma Bank (Iowa) for fly strains, clones and antibodies. I acknowledge Dr N. Brown (University of Cambridge, UK) for the cDNA library, Ajeet Pratap Singh and Abhijit Das for comments on the manuscript and help in making figures. The fusion construct for generation of the antibody was made by me in Prof G. Shaw's lab (University of Florida, USA). His help is gratefully acknowledged. This study was supported by the core funding from TIFR and the Extramural support from the Department of BioTechnology, government of India.

References

Arama E., Bader M., Rieckhof G. E. and Steller H. 2007 A ubiquitin ligase complex regulates caspase activation during sperm differentiation in *Drosophila. PLoS Biol.* **5**, e251.

Aso T., Yamazaki K., Aigaki T. and Kitajima S. 2000 *Drosophila* von Hippel-Lindau tumor suppressor complex possesses E3 ubiquitin ligase activity. *Biochem. Biophys. Res. Commun.* **276**, 355–361.

Atwood H. L., Govind C. K. and Wu C. F. 1993 Differential ultrastructure of synaptic terminals on ventral longitudinal abdominal muscles in *Drosophila* larvae. *J. Neurobiol.* **24**, 1008–1024.

Ayyub C., Sen A., Gonsalves F., Badrinath K., Bhandari P., Shashidhara L. S. *et al.* 2005 Cullin-5 plays multiple roles in cell fate specification and synapse formation during *Drosophila* development. *Dev. Dyn.* **232**, 865–875.

Babon J. J., Sabo J. K., Soetopo A., Yao S., Bailey M. F., Zhang J. G. *et al.* 2008 The SOCS box domain of SOCS3: structure and interaction with the elonginBC-cullin5 ubiquitin ligase. *J. Mol. Biol.* **381**, 928–940.

Budnik V., Zhong Y. and Wu C. F. 1990 Morphological plasticity of motor axons in *Drosophila* mutants with altered excitability. *J. Neurosci.* **10**, 3754–3768.

Ciechanover A., Orian A. and Schwartz A. L. 2000 Ubiquitin-mediated proteolysis: biological regulation via destruction. *Bioessays* **22**, 442–451.

Collins C. A., Wairkar Y. P., Johnson S. L. and DiAntonio A. 2006 Highwire restrains synaptic growth by attenuating a MAP kinase signal. *Neuron* **51**, 57–69.

DiAntonio A., Haghighi A. P., Portman S. L., Lee J. D., Amaranto A. M. and Goodman C. S. 2001 Ubiquitination-dependent mechanisms regulate synaptic growth and function. *Nature* **412**, 449–452.

Duan D. R., Pause A., Burgess W. H., Aso T., Chen D. Y. *et al.* 1995 Inhibition of transcription elongation by the VHL tumor suppressor protein. *Science* **269**, 1402–1406.

Estes P. S., Roos J., van Der Bliek A., Kelly R. B., Krishnan K. S. *et al.* 1996 Traffic of dynamin within individual *Drosophila* synaptic boutons relative to compartment-specific markers. *J. Neurosci.* **16**, 5443–5456.

Fay M. J., Longo K. A., Karathanasis G. A., Shope D. M., Mandernach C. J., Leong J. R. *et al.* 2003 Analysis of CUL-5 expression in breast epithelial cells, breast cancer cell lines, normal tissues and tumor tissues. *Mol. Cancer* **2**, 40.

Feldman R. M., Correll C. C., Kaplan K. B. and Deshaies R. J. 1997 A complex of Cdc4p, Skp1p, and Cdc53p/cullin catalyzes ubiquitination of the phosphorylated CDK inhibitor Sic1p. *Cell* **91**, 221–230.

Feng H., Zhong W., Punkosdy G., Gu S., Zhou L., Seabolt E. K. and Kipreos E. T. 1999 CUL-2 is required for the G1-to-S-phase transition and mitotic chromosome condensation in *Caenorhabditis elegans*. *Nat. Cell Biol*. **1**, 486–492.

Filippov V., Filippova M., Sehnal F. and Gill S. S. 2000 Temporal and spatial expression of the cell-cycle regulator cul-1 in *Drosophila* and its stimulation by radiation-induced apoptosis. *J. Exp. Biol.* **203**, 2747–2756.

Ghabrial A., Luschnig S., Metzstein M. M. and Krasnow M. A. 2003 Branching morphogenesis of the *Drosophila* tracheal system. *Annu. Rev. Cell Dev. Biol.* **19**, 623–647.

Glickman M. H. and Ciechanover A. 2002 The ubiquitin-proteasome proteolytic pathway: destruction for the sake of construction. *Physiol. Rev.* **82**, 373–428.

Gould A. P., Brookman J. J., Strutt D. I. and White R. A. 1990 Targets of homeotic gene control in *Drosophila*. *Nature* **348**, 308–312.

Gramates L. S. and Budnik V. 1999 Assembly and maturation of the *Drosophila* larval neuromuscular junction. *Int. Rev. Neurobiol.* **43**, 93–117.

Guan B., Hartmann B., Kho Y. H., Gorczyca M. and Budnik V. 1996 The *Drosophila* tumor suppressor gene, dlg, is involved in structural plasticity at a glutamatergic synapse. *Curr. Biol.* **6**, 695–706.

Hudson A. M. and Cooley L. 2010 *Drosophila* Kelch functions with Cullin-3 to organize the ring canal actin cytoskeleton. *J. Cell Biol.* **188**, 29–37.

Johansen J., Halpern M. E., Johansen K. M. and Keshishian H. 1989 Stereotypic morphology of glutamatergic synapses on identified muscle cells of *Drosophila* larvae. *J. Neurosci.* **9**, 710–725.

Kamura T., Maenaka K., Kotoshiba S., Matsumoto M., Kohda D. *et al.* 2004 VHL-box and SOCS-box domains determine binding specificity for Cul2-Rbx1 and Cul5-Rbx2 modules of ubiquitin ligases. *Genes Dev.* **18**, 3055–3065.

Kelso R. J., Hudson A. M. and Cooley L. 2002 *Drosophila* Kelch regulates actin organization via Src64-dependent tyrosine phosphorylation. *J. Cell Biol.* **156**, 703–713.

Keshishian H., Broadie K., Chiba A. and Bate M. 1996 The *Drosophila* neuromuscular junction: a model system for studying synaptic development and function. *Annu. Rev. Neurosci.* **19**, 545–575.

Kibel A., Iliopoulos O., Decaprio J. A. and Kaelin Jr W. G. 1995 Binding of the von Hippel-Lindau tumor suppressor protein to elongin B and C. *Science* **269**, 1444–1446.

Klambt C., Glazer L. and Shilo B. Z. 1992 Breathless, a *Drosophila* FGF receptor homolog, is essential for migration of tracheal and specific midline glial cells. *Genes Dev.* **6**, 1668–1678.

Koerner T. J., Hill J. E., Myers A. M. and Tzagoloff A. 1991 High-expression vectors with multiple cloning sites for construction of trpE fusion genes: pATH vectors. *Methods Enzymol.* **194**, 477–490.

Kugler J. M., Lem C. and Lasko P. 2010 Reduced cul-5 activity causes aberrant follicular morphogenesis and germ cell loss in *Drosophila* oogenesis. *PLoS ONE* **5**, e9048.

Lahey T., Gorczyca M., Jia X. X. and Budnik V. 1994 The *Drosophila* tumor suppressor gene dlg is required for normal synaptic bouton structure. *Neuron* **13**, 823–835.

Lisztwan J., Imbert G., Wirbelauer C., Gstaiger M. and Krek W. 1999 The von Hippel-Lindau tumor suppressor protein is a component of an E3 ubiquitin-protein ligase activity. *Genes Dev.* **13**, 1822–1833.

Maxwell P. H., Wiesener M. S., Chang G. W., Clifford S. C., Vaux E. C., Cockman M. E. *et al.* 1999 The tumour suppressor protein VHL targets hypoxia-inducible factors for oxygen-dependent proteolysis. *Nature* **399**, 271–275.

Mistry H., Wilson B. A., Roberts I. J., O'Kane C. J. and Skeath J. B. 2004 Cullin-3 regulates pattern formation, external sensory organ development and cell survival during *Drosophila* development. *Mech. Dev.* **121**, 1495–1507.

Mortimer N. T. and Moberg K. H. 2007 The *Drosophila* F-box protein Archipelago controls levels of the Trachealess transcription factor in the embryonic tracheal system. *Dev. Biol.* **312**, 560–571.

Muzzopappa M. and Wappner P. 2005 Multiple roles of the F-box protein Slimb in *Drosophila* egg chamber development. *Development* **132**, 2561–2571.

Ohlmeyer J. T. and Schupbach T. 2003 Encore facilitates SCF-Ubiquitin-proteasome-dependent proteolysis during *Drosophila* oogenesis. *Development* **130**, 6339–6349.

Ou C. Y., Lin Y. F., Chen Y. J. and Chien C. T. 2002 Distinct protein degradation mechanisms mediated by Cul1 and Cul3 controlling Ci stability in *Drosophila* eye development. *Genes Dev.* **16**, 2403–2414.

Ou C. Y., Pi H. and Chien C. T. 2003 Control of protein degradation by E3 ubiquitin ligases in *Drosophila* eye development. *Trends Genet.* **19**, 382–389.

Packard M., Koo E. S., Gorczyca M., Sharpe J., Cumberledge S. and Budnik V. 2002 The *Drosophila* Wnt, wingless, provides an essential signal for pre- and postsynaptic differentiation. *Cell* **111**, 319–330.

Querido E., Blanchette P., Yan Q., Kamura T., Morrison M., Boivin D. *et al.* 2001 Degradation of p53 by adenovirus E4orf6 and E1B55K proteins occurs via a novel mechanism involving a cullin-containing complex. *Genes Dev.* **15**, 3104–3117.

Ray K. and Rodrigues V. 1995 Cellular events during development of the olfactory sense organs in *Drosophila melanogaster*. *Dev. Biol.* **167**, 426–438.

Reynolds P. J., Simms J. R. and Duronio R. J. 2008 Identifying determinants of cullin binding specificity among the three functionally different *Drosophila melanogaster* Roc proteins via domain swapping. *PLoS ONE* **3**, e2918.

Samakovlis C., Hacohen N., Manning G., Sutherland D. C., Guillemin K. and Krasnow M. A. 1996a Development of the *Drosophila* tracheal system occurs by a series of morphologically distinct but genetically coupled branching events. *Development* **122**, 1395–1407.

Samakovlis C., Manning G., Steneberg P., Hacohen N., Cantera R. and Krasnow M. A. 1996b Genetic control of epithelial tube fusion during *Drosophila* tracheal development. *Development* **122**, 3531–3536.

Sasagawa Y., Sato S., Ogura T. and Higashitani A. 2007 *C. elegans* RBX-2-CUL-5- and RBX-1-CUL-2-based complexes are redundant for oogenesis and activation of the MAP kinase MPK-1. *FEBS Lett.* **581**, 145–150.

Schuster C. M., Davis G. W., Fetter R. D. and Goodman C. S. 1996 Genetic dissection of structural and functional components of synaptic plasticity. I. Fasciclin II controls synaptic stabilization and growth. *Neuron* **17**, 641–654.

Skowyra D., Craig K. L., Tyers M., Elledge S. J. and Harper J. W. 1997 F-box proteins are receptors that recruit phosphorylated substrates to the SCF ubiquitin-ligase complex. *Cell* **91**, 209–219.

Speese S. D., Trotta N., Rodesch C. K., Aravamudan B. and Broadie K. 2003 The ubiquitin proteasome system acutely regulates presynaptic protein turnover and synaptic efficacy. *Curr. Biol.* **13**, 899–910.

Spradling A. C. 1993 Developmental genetics of oogenesis. In *The development of Drosophila melanogaster,* vol 1 (ed. M. Bate and A. M. Arias) pp. 1–70. Cold Spring Harbor Laboratory Press, Plainview, USA.

Sutherland D., Samakovlis C. and Krasnow M. A. 1996 Branchless encodes a *Drosophila* FGF homolog that controls tracheal cell migration and the pattern of branching. *Cell* **87**, 1091–1101.

Tanaka-Matakatsu M., Uemura T., Oda H., Takeichi M. and Hayashi S. 1996 Cadherin-mediated cell adhesion and cell motility in *Drosophila* trachea regulated by the transcription factor Escargot. *Development* **122**, 3697–3705.

Van Dort C., Zhao P., Parmelee K., Capps B., Poel A., Listenberger L. *et al.* 2003 VACM-1, a cul-5 gene, inhibits cellular growth by a mechanism that involves MAPK and p53 signaling pathways. *Am. J. Physiol. Cell Physiol.* **285**, C1386–C1396.

van Roessel P., Elliott D. A., Robinson I. M., Prokop A. and Brand A. H. 2004 Independent regulation of synaptic size and activity by the anaphase-promoting complex. *Cell* **119**, 707–718.

Wan H. I., DiAntonio A., Fetter R. D., Bergstrom K., Strauss R. and Goodman C. S. 2000 Highwire regulates synaptic growth in *Drosophila*. *Neuron* **26**, 313–329.

Watts R. J., Hoopfer E. D. and Luo L. 2003 Axon pruning during *Drosophila* metamorphosis: evidence for local degeneration and requirement of the ubiquitin-proteasome system. *Neuron* **38**, 871–885.

Welchman R. L., Gordon C. and Mayer R. J. 2005 Ubiquitin and ubiquitin-like proteins as multifunctional signals. *Nat. Rev. Mol. Cell Biol.* **6**, 599–609.

Wu C., Wairkar Y. P., Collins C. A. and DiAntonio A. 2005 Highwire function at the *Drosophila* neuromuscular junction: spatial, structural, and temporal requirements. *J. Neurosci.* **25**, 9557–9566.

Zhao Y., Hegde A. N. and Martin K. C. 2003 The ubiquitin proteasome system functions as an inhibitory constraint on synaptic strengthening. *Curr. Biol.* **13**, 887–898.

Received 16 July 2010, in revised form 10 December 2010; accepted 17 January 2011
Published on the Web: 19 August 2011